



A Simple Fluorescent Probe for Sensing pH and its Application in *E. coli* Cells

Jianbin Chao¹ · Xiaolu Wang^{1,2} · Yongbin Zhang³ · Fangjun Huo³ · Caixia Yin⁴ · Miao Xu^{1,2}

Received: 27 December 2018 / Accepted: 19 March 2019 / Published online: 8 April 2019
© Springer Science+Business Media, LLC, part of Springer Nature 2019

Abstract

We designed and synthesized a simple fluorescent probe, (E)-2-(2-(3,4,5-Trimethoxybenzylidene)hydrazinyl) benzothiazole (probe), which could be applied to the detection of strongly acidic and alkaline pH in DMSO/water (1/4, v/v) system. It could be used to quantitatively detect strong acid in the range of 2.60–3.53 with a pK_a of 2.78. Meanwhile, it also showed an excellent linear relationship between the fluorescence intensity and alkaline pH values over the range of 9.98–10.95 with a pK_a of 9.32. The probe exhibited excellent properties to pH with high selectivity and sensitivity. The mechanism studies showed that the H⁺ binding with the N atom of benzothiazole moiety and hydrazine moiety in acid solution while the deprotonation of N atom in hydrazine group in basic environment. Importantly, the probe was successfully applied for imaging the strongly acidic and alkaline in *E. coli* cells.

Keywords Fluorescent probe · pH-sensitive · Extremely acid and alkaline · Bio-imaging

Introduction

For all we know, the pH plays a crucial role in biological systems. It is related with cell growth and division [1, 2], ion transport [3], endocytosis [4] and muscle contraction [5]. Therefore, it is vital to keep a appropriate pH for the normal cellular activities. For the human body, different part usually have different pH values, such as cytosol (pH 6.0–7.45) [6], saliva (pH 6.7–6.9) [7], lysosomes and endosomes (pH 4.5–6.0) [8], gastric juice (pH 2.0–3.0) [9]. Some diseases like

cancer, stroke and Alzheimer's disease are caused by abnormal pH values [10, 11]. So we are eager to develop a simple and accurate way to measure pH. In fact, there are many methods have been applied to measure the intracellular pH values such as acid-base indicator titration [12], pH-sensitive microelectrodes [13], ³¹P nuclear magnetic resonance technique [14]. However, these methods were time-consuming, destructive and easily interfered by environment factors [15]. Compared with these ways, fluorescent probes have attracted many successful applied in fluorescence imaging, medical diagnosis and other fields because its high sensitivity, good selectivity, and real-time detection [16–18].

Up to now, lots of fluorescent probes have been reported for pH, however, most of them are mainly for neutral pH (6–8) and weak acid pH (4–6) [6, 19, 20]. Only a few probes are designed for the extremely acid conditions (pH < 4) and extremely alkaline conditions (pH > 9) [21–24]. Although the strong acid or alkaline environment is not conducive to the survival of most organisms, some microorganisms such as *Helicobacter pylori*, eosinophilic bacteria and basophilic bacteria prefer living in this environment [25–27]. And, mammals also have very acidic physiological environments, such as gastric juice, which abnormal pH value lead to gastric dysfunction and directly cause of stomach diseases [26, 28]. For these reasons, it is necessary to develop a fluorescence sensor to detect the strong acid and alkaline.

Electronic supplementary material The online version of this article (<https://doi.org/10.1007/s10895-019-02368-2>) contains supplementary material, which is available to authorized users.

✉ Jianbin Chao
chao@sxu.edu.cn

- ¹ Scientific Instrument Center, Shanxi University, Taiyuan 030006, China
- ² School of Chemistry and Chemical Engineering, Shanxi University, Taiyuan 030006, China
- ³ Research Institute of Applied Chemistry, Shanxi University, Taiyuan 030006, China
- ⁴ Institute of Molecular Science, Shanxi University, Taiyuan 030006, China

The benzothiazole group possess good fluorescence properties owing to their large range of π -conjugated systems. And it is always regarded as fluorophore and recognition moiety due to it contains two heteroatoms (N and S) that can be coordinated with metal ions [29, 30]. Many fluorescent probes based on benzothiazole have been reported in recent years. Liu reported a fluorescent probe for Fe^{3+} based on 2-(2-hydroxyphenyl)benzothiazole [31], Nguyen designed a benzothiazole-based fluorescent probe for hypochlorous acid [32]. Zhang synthesized a probe based on the iminocoumarin benzothiazole for sensing hydrogen sulfide [33]. Shen designed a simple fluorescent probe based on a benzothiazole derivative that can be used to detect for copper and biothiols [34]. In this paper, we designed a simple probe, (E)-2-(2-(3,4,5-Trimethoxybenzylidene)hydrazinyl)benzothiazole (probe), which was constructed via benzothiazole and 3,4,5-trimethoxy benzene. The probe can be used to detect the extreme acid and alkaline with high sensitivity and good selectivity. The fluorescence intensity showed an excellent linear relationship with pH value over the range of 2.60–3.53 and 9.98–10.95. And the cells imaging studies revealed that probe had a great potential to monitor pH change in *E. coli* cells.

Experimental Section

Materials and Instrumentation

All reagents and solvents were commercially available (Sinopharm Chemical Reagent Beijing Co., Ltd.). The solvents and chemicals were analytical grade and used without further purification unless for special needs. Distilled water was used throughout the process of UV-vis and fluorescence measurements.

^1H NMR and ^{13}C NMR experiments were taken on a Bruker AVANCE-600 MHz and 150 MHz NMR spectrometer, respectively. HRMS data were achieved with a Thermo Scientific Q Exactive LC-MS/MS system. All pH was controlled by a PHS-3C digital pH-meter (YouKe, China). Absorption spectra were obtained by a UV-2450 spectrophotometer (Shimadzu, Japan). Fluorescence measurements were recorded on a F-7000 fluorescence spectrophotometer

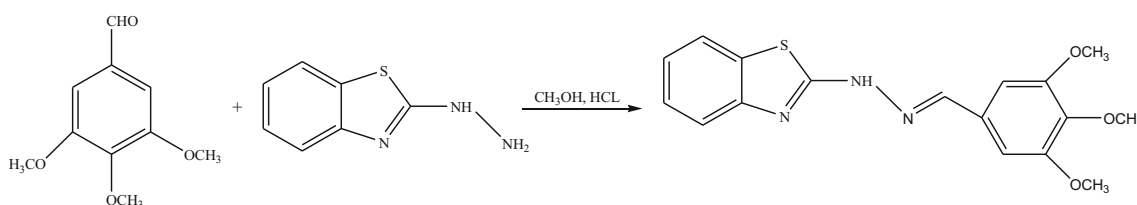
(Hitachi, Japan). Imaging in *E. coli* cells was conducted on a ZEISS LSM 880 confocal laser scanning microscope.

Synthesis of (E)-2-(2-(3,4,5-Trimethoxybenzylidene)hydrazinyl) Benzothiazole (Probe)

2-hydrazinobenzothiazole (0.33 g, 30 mM) and 3,4,5-trimethoxybenzaldehyde (0.40 g, 30 mM) were added into a 250 mL three-neck round bottom flask and dissolved completely in anhydrous methanol (65.0 mL). Added 3–4 drops concentrated hydrochloric acid to the mixture and stirred it at room temperature. After 2 h, added 2–3 drops concentrated hydrochloric acid to the solution and kept stirring it for 18 h. Then the resulting solution was heated to reflux for 5 h. The reaction was monitored by TLC ($V_{\text{ethyl acetate}}: V_{\text{petroleum ether}} = 2: 1$). After cooled down to room temperature, the solid was filtered off under reduced pressure and washed with methanol for three times and dried in vacuum to afford probe (0.53 g, 76.8%, Scheme 1). The structure of probe was characterized by ^1H NMR and ^{13}C NMR. ^1H NMR (DMSO- d_6 , 600 MHz, δ/ppm): 8.12 (s, 1H), 7.81 (d, $J = 7.6$ Hz, 1H), 7.47 (d, $J = 6.8$ Hz, 1H), 7.34–7.31 (t, $J = 7.5$ Hz, 1H), 7.15–7.13 (t, $J = 7.3$ Hz, 1H), 7.06 (s, 2H), 3.85 (s, 6H), 3.71 (s, 3H), (Fig. S1). ^{13}C NMR (DMSO- d_6 , 150 MHz, δ/ppm): 167.06, 153.67, 146.82, 139.77, 129.74, 127.75, 127.04, 123.12, 122.70, 117.09, 104.81, 60.61, 56.44, 49.05 (Fig. S2).

Sample Preparation and Spectroscopic Measurements

Dissolved the probe in DMSO as the stock solutions (1.0 mM). We diluted the stock solution to 10.0 μM with DMSO/water (1/4, V/V) for fluorescence and UV-vis measurement. Absorption and fluorescence spectra were measured with 1.0-cm quartz cells. A series of ions solutions (K^+ , Na^+ , Ca^{2+} , Zn^{2+} , Mg^{2+} , Al^{3+} , Co^{2+} , Cr^{3+} , Ni^{2+} , Bi^{3+} , Cu^{2+} , Hg^{2+} , Fe^{2+} , Fe^{3+} , Pb^{2+} and Mn^{2+}) for anti-interference tests were prepared from the corresponding hydrochloride salts. The solutions of common amino acids (Phe, Asp, Ala, Leu, Lys, Val, Ser, Gly) prepared in redistilled water. The excitation wavelength was set at 355 nm (slit: 5 nm/10 nm) for the fluorescence measurements.



Scheme 1 Synthetic routes of probe

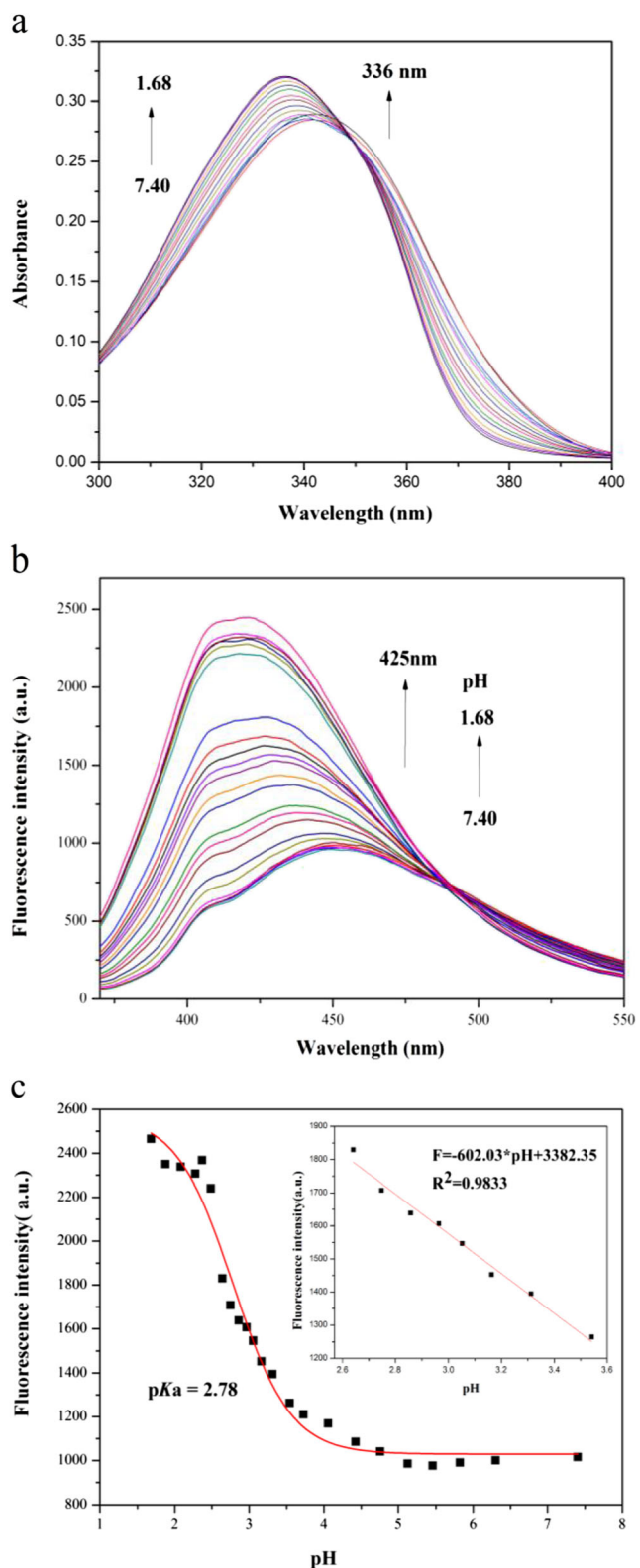


Fig. 1 **a** Absorption and **b** fluorescence spectra ($\lambda_{ex} = 355$ nm, slit = 5/10 nm) of 10.0 μ M probe in DMSO/water (1/4, V/V) at different pH value (from 7.40 to 1.68); **c** plot of the emission fluorescence intensity of probe at 425 nm at various pH values. The inset showed the linear relationship of fluorescence intensity at 425 nm and pH values from 2.60 to 3.53

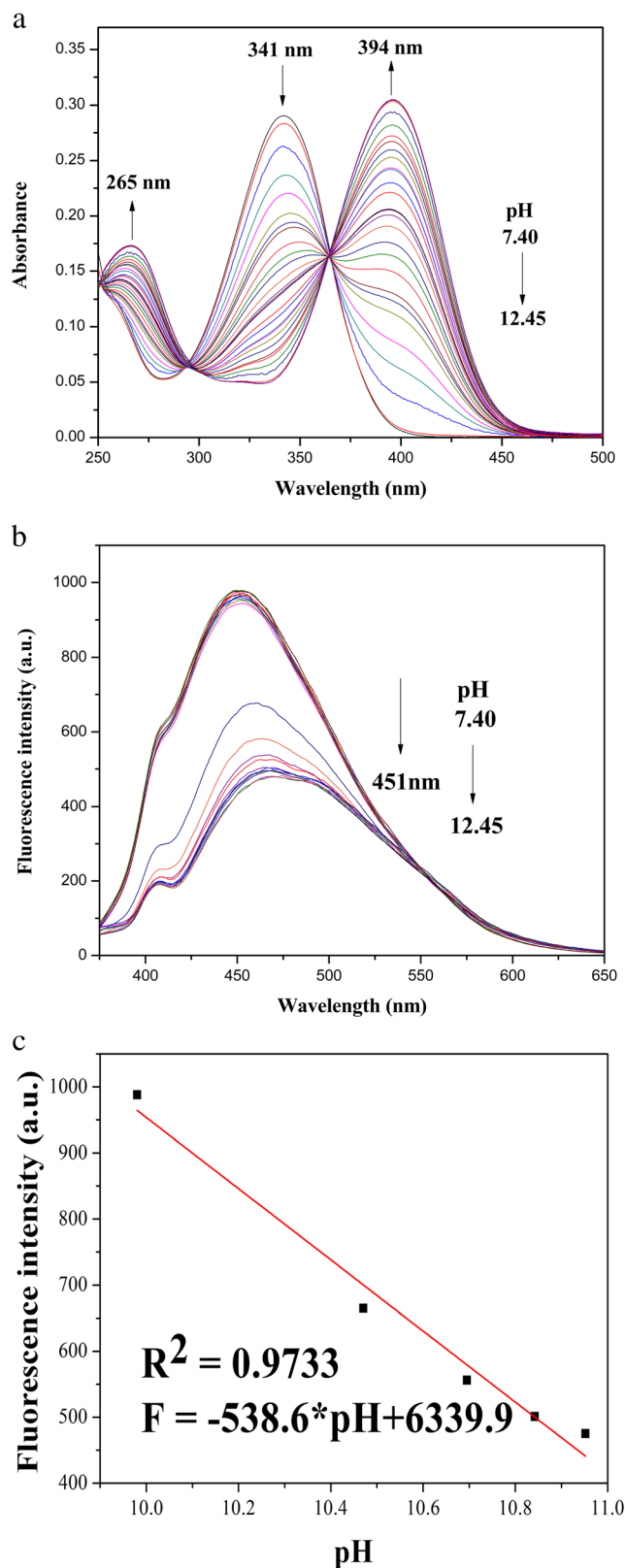


Fig. 2 **a** UV-vis and **b** fluorescence spectra ($\lambda_{ex} = 355$ nm, slit = 5/10 nm) of 10.0 μ M probe in DMSO/water (1/4, V/V) at different pH value (from 7.40 to 12.45); **c** plot of the emission fluorescence intensity of probe at 451 nm at various pH values. The inset showed the linear relationship of fluorescence intensity at 451 nm and pH values from 9.98 to 10.95

Bacteria Culture and Imaging

E. coli strains were inoculated into Luria-Bertani (LB) culture medium (NaCl 10 g/L, Trptone 10 g/L and yeast extract 5 g/L) and incubated at 37 °C in a table concentrator at 180 rpm for 15 h. Next, the bacteria were equally divided into nine centrifuge tubes and collected by centrifugation at 4300 rpm for 5 min. The sediment was washed three times and resuspended with various pH solutions (11.00, 10.60, 10.30, 9.00, 7.40, 5.50, 3.00, 2.50, 1.70), respectively. After 10 min, every tube was added with probe to make the final concentration of probe to be 20 μM and incubated in a table concentrator for 2 h at 37 °C. Before imaging, the *E. coli* cells were washed twice with distilled water.

Results and Discussion

Spectroscopic Properties of Probe

The UV-vis absorption spectra of 10.0 μM probe were discussed in DMSO/water (1/4, V/V) at various pH values. At neutral condition, probe exhibited a maximum absorption at 341 nm ($\epsilon = 2.89 \times 10^4$), however, the absorption peak enhanced and blue-shifted to 336 nm ($\epsilon = 3.21 \times 10^4$) upon adding the environmental acidity from pH 7.40 to 1.68 (Fig. 1a). When the alkalinity of solution increased from pH 7.40 to 12.45, the peak at 341 nm significantly decreased accompanied by the appearance of two new peaks centred at 265 nm and 394 nm (Fig. 2a).

Next, the fluorescence changes of probe (10 μM) in different pH environment were studied. As seen from the Fig. 1b, the probe fluorescence intensity at 451 nm increased and blue-shifted to 425 nm with the lowering the pH from 7.40 to 1.68. The fluorescence emission intensity at 425 nm ($F_{425 \text{ nm}}$) versus pH showed “S” shaped calibration graph with a pK_a of 2.78 (Fig. 1c). Besides, there was a great linear relationship between the $F_{425 \text{ nm}}$ and pH values from 2.60 to 3.53 with the linear equation $F_{425 \text{ nm}} = -592.8 \cdot \text{pH} + 3353.8$ (inset of Fig. 1c, $R^2 = 0.9833$). With increasing the environmental basicity from 7.40 to 12.45, the fluorescence intensity at 451 nm ($F_{451 \text{ nm}}$) decreased remarkably (Fig. 2b). From the sigmoidal plot of the $F_{451 \text{ nm}}$ with pH value, a pK_a value of 9.32 was calculated which implied the probe was sensitive around this pH values (Fig. 2c). Concomitantly, the $F_{451 \text{ nm}}$ displayed a good linear correction with pH in the range of 9.98–10.95 with the function of $F_{451 \text{ nm}} = -538.6 \cdot \text{pH} + 6339.9$, $R^2 = 0.9733$ (inset of Fig. 2c). These linear curves make it easier to quantitative determination of pH over this pH range.

The Selectivity of Probe

Taking into account the intracellular environment was complex, we evaluated the anti-interference capacity of 10.0 μM probe to pH at pH 8.20, 7.40 and 2.75 by an anti-interference test, respectively. The influence of various metal cations (K^+ , Na^+ , Ca^{2+} , Zn^{2+} , Mg^{2+} , Al^{3+} , Co^{2+} , Cr^{3+} , Ni^{2+} , Bi^{3+} , Cu^{2+} , Hg^{2+} , Fe^{2+} , Fe^{3+} , Pb^{2+} and Mn^{2+}) and some common amino acids (Phe, Asp, Ala, Leu, Lys, Val, Ser, Gly) on the fluorescence intensity of probe were shown in Fig. 3 and Fig. S3. They all didn't cause visible effect on the pH response of probe. From the experimental results, we could conclude that

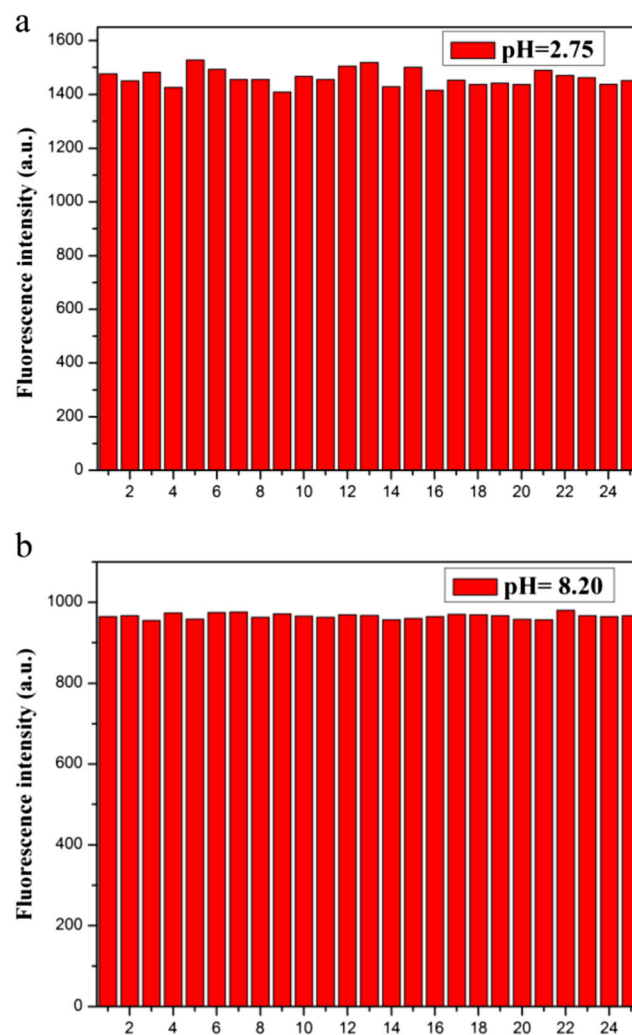


Fig. 3 Fluorescence changes of 10.0 μM probe in DMSO/water (1/4, V/V) toward various metal ions and common amino acids ($\lambda_{\text{ex}} = 355 \text{ nm}$, slits = 5/10 nm). **a** pH 2.75, $\lambda_{\text{em}} = 425 \text{ nm}$; **b** pH 8.20, $\lambda_{\text{em}} = 451 \text{ nm}$. 1. Blank; 2. K^+ (25 mM); 3. Na^+ (25 mM); 4. Ca^{2+} (5 mM); 5. Zn^{2+} ; 6. Mg^{2+} ; 7. Al^{3+} ; 8. Co^{2+} ; 9. Cr^{2+} ; 10. Ni^{2+} ; 11. Bi^{3+} ; 12. Cu^{2+} (0.1 mM); 13. Hg^{2+} ; 14. Fe^{2+} (0.1 mM); 15. Fe^{3+} (0.05 mM); 16. Pb^{2+} ; 17. Mn^{2+} ; 18. Phe (5 μM); 19. Asp (5 μM); 20. Ala (5 μM); 21. Leu (5 μM); 22. Lys (5 μM); 23. Val (5 μM); 24. Ser (5 μM); 25. Gly (5 μM); other unlabeled ions: 0.2 mM

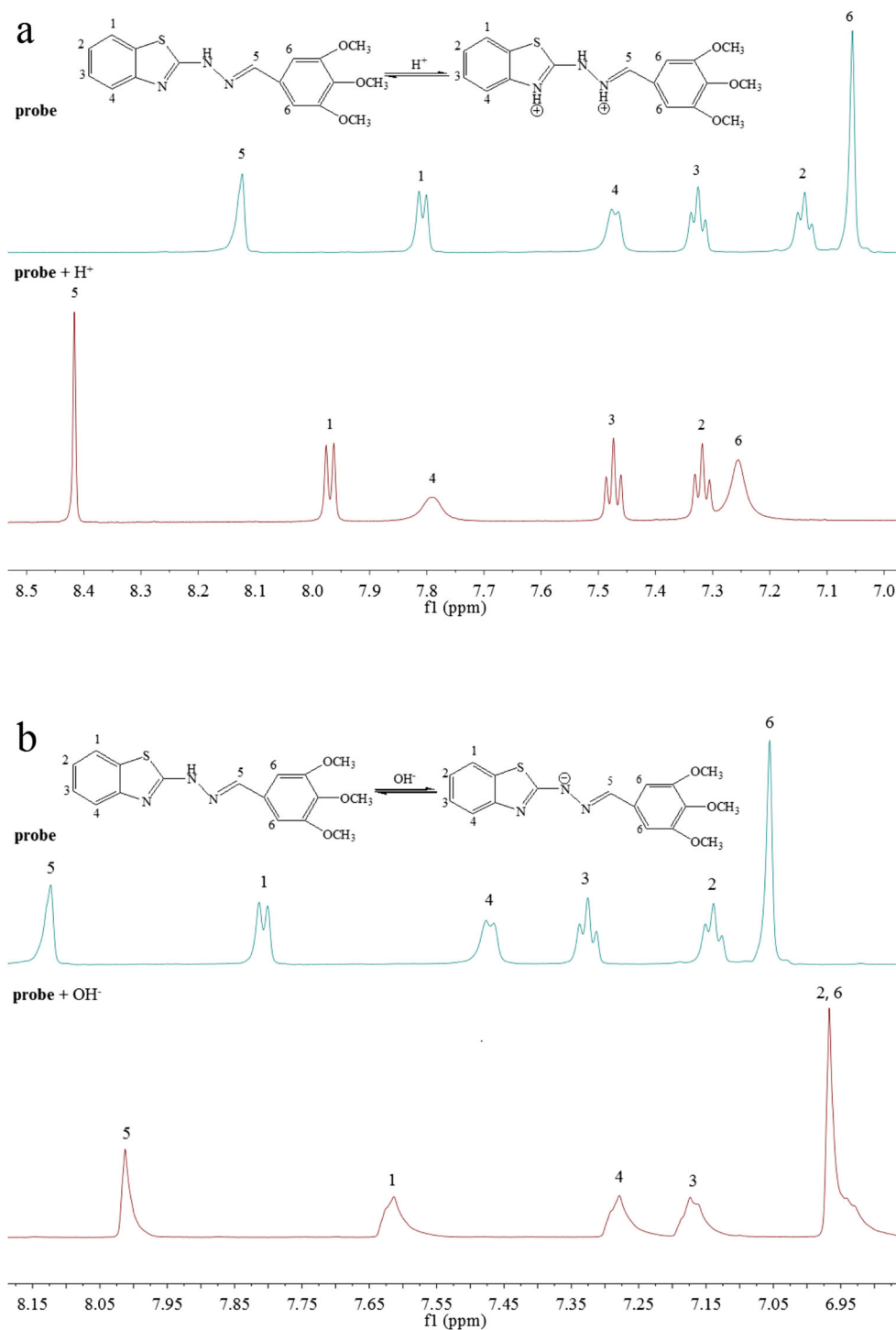
probe had the ability to detect pH selectivity in complex intracellular environment.

Photostability and Reversibility

The time courses of the fluorescence intensity of probe (10.0 μM) at pH 1.68, 2.75, 10.51 and 13.04 were studied. Figure S4 exhibited the reaction of probe to pH could be

finished within 5 min. And the fluorescence intensity kept unchanged during 2 h, indicating probe had good photostability and was appropriate for real-time monitoring pH. The reversibility was another very vital character for fluorescent probes. Thus, the reversibility experiment of probe towards pH was carried out. The fluorescence intensities of probe were recorded when the pH of solution was adjusted back and forth between 7.40 and 12.45 four times. As shown

Fig. 4 **a** Partial ^1H NMR spectra of probe and probe + H^+ in DMSO-d_6 . **b** Partial ^1H NMR spectra of probe and probe + OH^- in DMSO-d_6



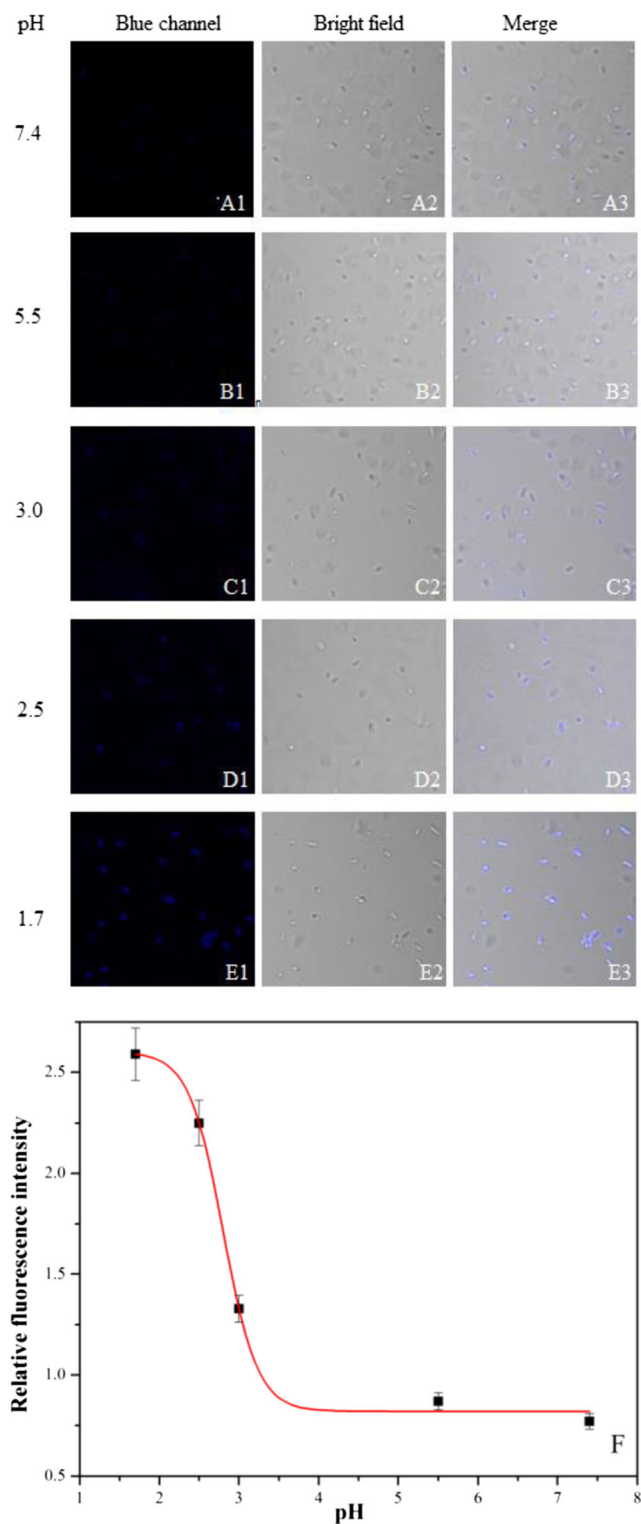


Fig. 5 Imaging acidity in *E. coli* cells with probe (20.0 μ M). A: pH 7.4; B: pH 5.5; C: pH 3.0; D: pH 2.50; E: pH 1.7. First column: blue channel (410–500 nm, λ_{ex} = 405 nm); second column: bright field; third column: overlapped of blue channel and bright field. F: The relative fluorescence intensity of *E. coli* cells incubated in different pH buffer

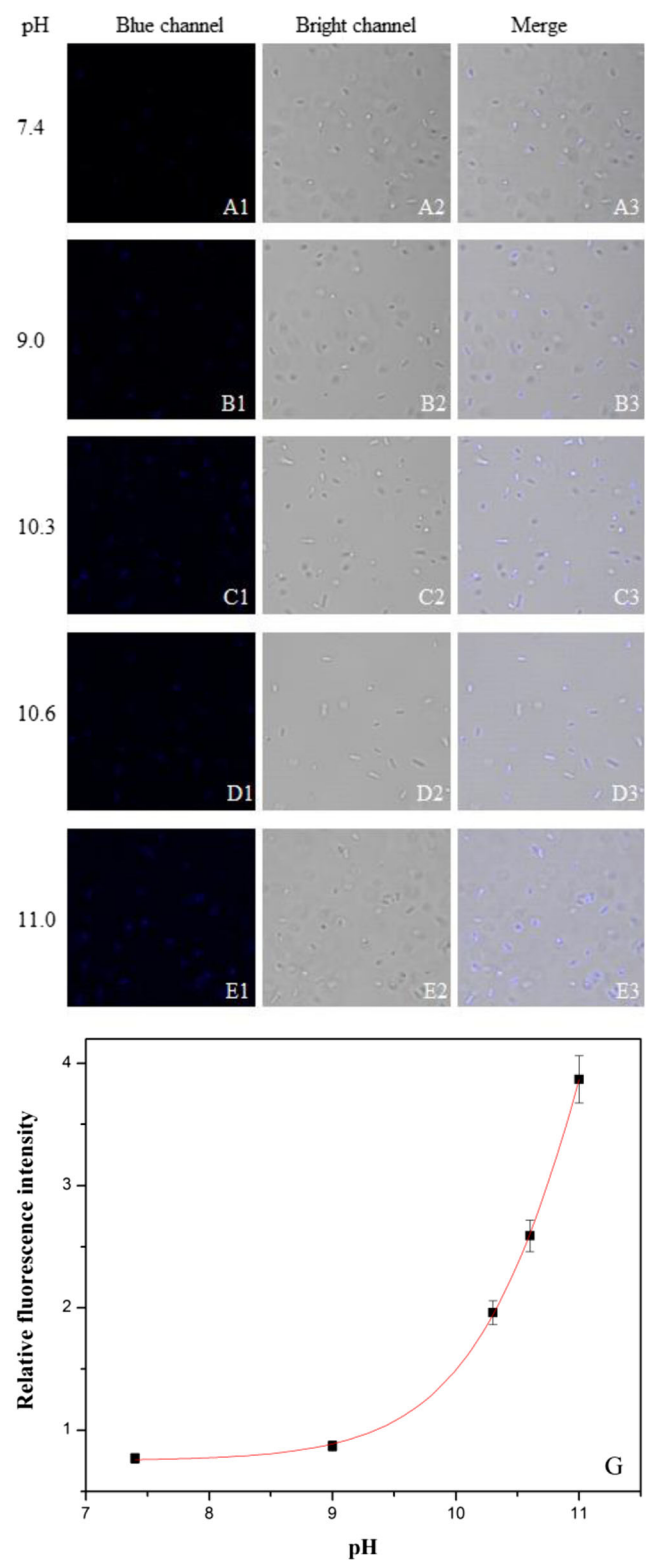


Fig. 6 Imaging alkalinity in *E. coli* cells of probe (20.0 μ M). A: pH 7.40; B: pH 9.0; C: pH 10.3; D: pH 10.6; E: pH 11.0. First column: blue channel (410–500 nm, λ_{ex} = 405 nm); second column: bright field; third column: overlapped of blue channel and bright field. G: The relative fluorescence intensity of *E. coli* cells incubated at different pH buffer

in Fig. S5, the probe was fully reversible in basic circumstance, and the response and recovery times are rapid within seconds. Therefore, the probe could detect the base in real time.

Proposed Mechanism of the pH Response of Probe

We speculated that the fluorescence and absorption changes of probe could owing to the intramolecular charge transfer (ICT) mechanism from the benzothiazole (electron-donor) to the methoxy benzene moiety (electron-acceptor). To further provide direct evidence for the sensing mechanism between the probe and pH, ^1H NMR experiment was conducted in d_6 -DMSO (Fig. 4). In the presence of HCl, the chemical shifts of the benzothiazole ring protons (H-1, H-2, H-3 and H-4) were downfield shift, which indicated that H^+ have been binding with nitrogen atom of the benzothiazol. At the same time, the protons of methoxy benzene moiety (H-6) and H-5 showed downfield shift, which implied that the protonation of hydrazine nitrogen atom. The reason why these protons down-shifted was that the binding of H^+ and N atom led to the decrease in the charge density around these protons. At the same time, the protonation of nitrogen atom led to a decrease of the ability of benzothiazole giving electrons. Upon the addition of NaOH, the chemical shifts of all protons were up-field shifted as shown in Fig. 4b, which indicated that the deprotonation of N atom in hydrazine group.

Fluorescence Imaging pH in *E. coli* Cells

In order to access the potential application of probe for pH detecting in living sample, *E. coli* cells were employed to image the pH change. To create acid and alkaline surroundings for bacteria, we used buffer with pH 11.0, 10.6, 10.3, 9.00, 7.40, 5.50, 3.00, 2.50 and 1.70, respectively, to incubate *E. coli*. As seen from the Fig. 5, the *E. coli* cells exhibited weak blue fluorescence (410–500 nm, $\lambda_{\text{ex}} = 405$ nm) at pH 7.40, but it enhanced gradually with reduction of the H^+ concentration from 7.40 to 1.70. When the environmental alkaline changed from 7.40 to 11.00, the fluorescence in blue channel enhanced obviously (Fig. 6). The variation of relative fluorescence intensity in blue channel under different pH value were shown in Figs. 5f and 6g. These results were in agreement with the changes of the fluorescence at $\lambda_{\text{ex}} = 405$ nm that showed in Fig. S6. Meanwhile, we affirmed that *E. coli* cells could survive in such extremely acidic or alkaline circumstance, and the probe was suitable for monitoring such alkaline and acidic extracellular pH changes.

Conclusion

In summary, we reported a simple probe that could be used to detect the extreme acidic and alkaline. The probe displayed a “turn on” fluorescence respond in acid solutions and had a linearly relationship with pH value in the range of 2.60–3.53 with a pK_a 2.78. However, it exhibited a “turn off” response to basic at the $\lambda_{\text{ex}} = 355$ nm and the linear range was 9.98–10.95. The probe possesses excellent photostability, good selectivity and cell membrane permeability. And the probe exhibited reversible in basic environment. The mechanism was verified to protonation and deprotonation of N atom by the ^1H NMR spectra. Most importantly, the application of probe to image pH in bacteria was realized successfully. Based on the great properties of probe, we confirmed that the probe would be an efficient tool for imaging pH distribution and change tracking.

Acknowledgements The work was supported by the National Natural Science Foundation of China (No. 21472118, 21672131), the Program for the Top Young and Middle-aged Innovative Talents of Higher Learning Institutions of Shanxi (No. 2013802), Talents Support Program of Shanxi Province (No. 2014401), Shanxi Province Outstanding Youth Fund (No. 2014021002), Natural Science Foundation of Shanxi Province of China (No. 201701D121018).

References

- Gottlieb RA, Nordberg J, Skowronski E, Babior BM (1996) Apoptosis induced in Jurkat cells by several agents is preceded by intracellular acidification. *Proc Natl Acad Sci U S A* 93:654–658
- Gottlieb RA, Giesing HA, Zhu JY, Engler RL, Babior BM (1995) Cell acidification in apoptosis: granulocyte colony-stimulating factor delays programmed cell death in neutrophils by up-regulating the vacuolar H^+ -ATPase. *Proc Natl Acad Sci U S A* 92:5965–5968
- Hoyt KR, Reynolds IJ (1998) Alkalinization prolongs recovery from glutamate-induced increases in intracellular Ca^{2+} concentration by enhancing Ca^{2+} efflux through the mitochondrial $\text{Na}^+/\text{Ca}^{2+}$ exchanger in cultured rat forebrain neurons. *J Neurochem* 71:1051–1058
- Blott EJ, Griffiths GM (2002) Secretory lysosomes. *Nat Rev Mol Cell Biol* 3:122–131
- Edmonds BT, Murray J, Condeelis J (1995) pH regulation of the F-actin binding properties of Dictyostelium elongation factor 1 alpha. *J Biol Chem* 270:15222–15230
- Sun KM, McLaughlin CK, Lantero DR, Manderville RA (2007) Biomarkers for phenol carcinogen exposure act as pH-sensing fluorescent probes. *J Am Chem Soc* 129:1894–1895
- Jr LR, Bentley CD, Haywood VB (1994) Salivary pH changes during 10% carbamide peroxide bleaching. *Quintessence Int* 25: 547–550
- Galindo F, Burguete MI, Vigarra L, Luis SV, Kabir N, Gavrilovic J, Russell DA (2005) Synthetic macrocyclic peptidomimetics as tunable pH probes for the fluorescence imaging of acidic organelles in live cells. *Angew Chem* 117:6662–6666

9. Zhang WJ, Fan L, Li ZB, Ou T, Zhai HJ, Yang J, Dong C, Shuang SM (2016) Thiazole-based ratiometric fluorescence pH probe with large Stokes shift for intracellular imaging. *Sensors Actuators B Chem* 233:566–573
10. Davies TA, Fine RE, Johnson RJ, Levesque CA, Rathbun WH, Seetoo KF, Smith SJ, Strohmeier G, Volicer L, Delva L (1993) Non-age related differences in thrombin responses by platelets from male patients with advanced Alzheimer's disease. *Biochem Biophys Res Commun* 194:537–543
11. Izumi H, Torigoe T, Ishiguchi H, Uramoto H, Yoshida Y, Tanabe M, Ise T, Murakami T, Yoshida T, Nomoto M (2003) Cellular pH regulators: potentially promising molecular targets for cancer chemotherapy. *Cancer Treat Rev* 29:541–549
12. Spanswick RM, Miller AG (1977) Measurement of the cytoplasmic pH in *Nitella translucens*. Comparison of values obtained by microelectrode and weak acid methods. *Plant Physiol* 59:664–666
13. Antoneko YN, Bulychev AA (1991) Measurements of local pH changes near bilayer lipid membrane by means of a pH microelectrode and a protonophore-dependent membrane potential. Comparison of the methods. *Biochim Biophys Acta Biomembr* 1070:279–282
14. Seo Y, Murakami M, Watari H, Imai Y, Yoshizaki K, Nishikawa H, Morimoto T (1983) Intracellular pH determination by a ^{31}P -NMR technique. The second dissociation constant of phosphoric acid in a biological system. *Magn Reson Imaging* 2:147–147
15. Slavik J (1982) Intracellular pH of yeast cells measured with fluorescent probes. *FEBS Lett* 140:22–26
16. Shi W, Li X, Ma H (2014) Fluorescent probes and nanoparticles for intracellular sensing of pH values. *Methods Appl Fluoresc* 2:042001
17. Wang J, Vernier PT, Sun Y, Marcu L (2005) A fluorescence microscopy study of quantum dots as fluorescent probes for brain tumor diagnosis. *Proc SPIE* 5703:127–134
18. Winkler AM, Rice PFS, Barton JK (2009) In vivo imaging using a VEGF-based near-infrared fluorescent probe for early cancer diagnosis in the AOM-treated mouse model. *Proc SPIE* 7190:71900M–71900M-9
19. Cui DW, Qian XH, Liu FY, Zhang R (2004) Novel fluorescent pH sensors based on intramolecular hydrogen bonding ability of naphthalimide. *Org Lett* 6:2757–2760
20. Wan Q, Chen S, Shi W, Li L, Ma H (2015) Lysosomal pH rise during heat shock monitored by a lysosome-targeting near-infrared ratiometric fluorescent probe. *Angew Chem* 126:11096–11100
21. Chao JB, Wang HJ, Zhang YB, Yin CX, Huo FJ, Song KL, Li ZQ, Zhang T, Zhao Y (2017) A novel “donor- π -acceptor” type fluorescence probe for sensing pH: mechanism and application in vivo. *Talanta* 174:468–476
22. Xu Y, Jiang Z, Xiao Y, Bi FZ, Miao JY, Zhao BX (2014) A new fluorescent pH probe for extremely acidic conditions. *Anal Chim Acta* 820:146–151
23. Zhang X, Jing SY, Huang SY, Zhou XW, Bai JM, Zhao BX (2015) New fluorescent pH probes for acid conditions. *Sensors Actuators B Chem* 206:663–670
24. Niu W, Fan L, Nan M, Wong MS, Shuang SM, Dong C (2016) A novel fluorescent probe for sensing and imaging extreme acidity. *Sensors Actuators B Chem* 234:534–540
25. Krulwich TA, Sachs G, Padan E (2011) Molecular aspects of bacterial pH sensing and homeostasis. *Nat Rev Microbiol* 9:330–343
26. Merrell DS, Camilli A (2002) Acid tolerance of gastrointestinal pathogens. *Curr Opin Microbiol* 5:51–55
27. Ferguson BJ, Seethala R, Wood WA (2007) Eosinophilic bacterial chronic rhinosinusitis. *Laryngoscope* 117:2036–2040
28. HE MS, Li Z (2012) Study on the influence of folic acid for the gastric juice pH value of helicobacter pylori positive patients with chronic atrophic gastritis. *National Medical Frontiers of China* 7:24–25
29. Nas A, Dilber G, Durmus M, Kantekin H (2015) The influence of the various central metals on photophysical and photochemical properties of benzothiazole-substituted phthalocyanines. *Spectrochim Acta A* 135:55–62
30. Wagh YB, Kuwar A, Sahoo SK, Gallucci J, Dalal DS (2015) Highly selective fluorimetric sensor for Cu^{2+} and Hg^{2+} using a benzothiazole-based receptor in semi-aqueous media and molecular docking studies. *RSC Adv* 5:45528–45534
31. Liu SD, Zhang LW, Liu X (2013) A highly sensitive and selective fluorescent probe for Fe^{3+} based on 2-(2-hydroxyphenyl)benzothiazole. *New J Chem* 37:821–826
32. Nguyen KH, Hao Y, Zeng K, Fan S, Li F, Yuan S, Ding X, Xu M, Liu YN (2018) A benzothiazole-based fluorescent probe for hypochlorous acid detection and imaging in living cells. *Spectrochim Acta A* 199:189–193
33. Zhang H, Xie Y, Wang P, Chen G, Liu R, Lam YW, Hu Y, Zhu Q, Sun H (2015) An iminocoumarin benzothiazole-based fluorescent probe for imaging hydrogen sulfide in living cells. *Talanta* 135:149–154
34. Shen Y, Zhang X, Zhang C, Zhang Y, Jin J, Li H (2018) A simple fluorescent probe for the fast sequential detection of copper and biothiols based on a benzothiazole derivative. *Spectrochim Acta A* 191:427–434

Publisher's Note Springer Nature remains neutral with regard to jurisdictional claims in published maps and institutional affiliations.